REGULAR ARTICLE

blood advances

Unexpected redundancy of Gpr56 and Gpr97 during hematopoietic cell development and differentiation

Antonio Maglitto,[1,*] Samanta A. Mariani,[1,*] Emma de Pater,[2] Carmen Rodriguez-Seoane,[1] Chris S. Vink,[1] Xianhua Piao,[3] Mari-Liis Lukke,[1] and Elaine Dzierzak[1]

[1]Centre for Inflammation Research, The University of Edinburgh, Edinburgh, United Kingdom; [2]Department of Hematology, Erasmus Medical Center, Rotterdam, The Netherlands; and [3]Newborn Brain Research Institute, Department of Pediatrics, University of California San Francisco, San Francisco, CA

Key Points

- Lineage output of mouse fetal liver HSC is dependent on Gpr56; on *Gpr56* deletion, *Gpr97* is upregulated and HSC myeloid bias increases.
- Mouse *Gpr97* rescues HS/PC generation in *gpr56* morphant zebrafish; deletion of both *Gpr56* and *Gpr97* in mouse ESC abolishes HPC production.

Integrated molecular signals regulate cell fate decisions in the embryonic aortic endothelium to drive hematopoietic stem cell (HSC) generation during development. The G-protein–coupled receptor 56 (*Gpr56*, also called *Adgrg1*) is the most highly upregulated receptor gene in cells that take on hematopoietic fate and is expressed by adult bone marrow HSCs. Despite the requirement for *Gpr56* in hematopoietic stem/progenitor cell (HS/PC) generation in zebrafish embryos and the highly upregulated expression of *GPR56* in treatment-resistant leukemic patients, its function in normal mammalian hematopoiesis remains unclear. Here, we examine the role of Gpr56 in HS/PC development in *Gpr56* conditional knockout (cKO) mouse embryos and *Gpr* knockout (KO) embryonic stem cell (ESC) hematopoietic differentiation cultures. Our results show a bias toward myeloid differentiation of *Gpr56* cKO fetal liver HSCs and an increased definitive myeloid progenitor cell frequency in $Gpr56^{KO}$ ESC differentiation cultures. Surprisingly, we find that mouse *Gpr97* can rescue *Gpr56* morphant zebrafish hematopoietic generation, and that *Gpr97* expression is upregulated in mouse *Gpr56* deletion models. When both *Gpr56* and *Gpr97* are deleted in ESCs, no or few hematopoietic PCs (HPCs) are generated upon ESC differentiation. Together, our results reveal novel and redundant functions for these 2 G-protein coupled receptors in normal mammalian hematopoietic cell development and differentiation.

Introduction

Hematopoietic stem cells (HSCs) are rare, self-renewing cells that sustain lifelong blood production. In vertebrate embryos, HSCs arise in the aorta-gonad mesonephros (AGM) region from hemogenic endothelial cells that undergo a highly conserved "endothelial-to-hematopoietic transition" (EHT) process.[1-4] Transcriptomics and loss-of-function studies have identified candidate regulators in transitioning cells.[5-11]

We identified *Gpr56* as the highest upregulated receptor gene during mouse EHT and localized its expression to emerging hematopoietic cells.[12] Gpr56 is an adhesion G-protein–coupled receptor that mediates cell–cell and cell–matrix interactions.[13] It is well-conserved across vertebrate species and contains 4 domains (external-*N*-terminal, GPCR-autoproteolysis-Inducing, 7-transmembrane, C-terminal-cytoplasmic).[14] Upon ligand-binding, an autoproteolytic cleavage divides the protein in 2 noncovalently linked fragments. The cytoplasmic domain signals through RhoA/ROCK to trigger downstream cellular functions.[15-17]

Submitted 26 October 2020; accepted 1 December 2020; published online 5 February 2020. DOI 10.1182/bloodadvances.2020003693.

*A.M. and S.A.M. are joint first authors and contributed equally to this work.

Send data sharing requests via e-mail to the corresponding authors, Samanta A. Mariani (s.mariani@ed.ac.uk) and Elaine Dzierzak (elaine.dzierzak@ed.ac.uk).

The full-text version of this article contains a data supplement.

Gpr56 function is well-characterized in central nervous system (CNS) development and its dysfunction is linked to human genetic disorders. *Gpr56* deletion in the mouse causes a severe reduction in CNS myelination,[16,18] and mutations in human GPR56 cause a recessive brain malformation, defective cerebral cortex, and CNS hypomyelination.[19,20] Interestingly, aberrant expression of GPR56 in leukemic stem cells is associated with high-risk/treatment resistance in patients with AML.[21-24] However, its role in normal hematopoiesis is uncertain.

Gpr56 knockdown zebrafish embryos suffer dramatic reductions in aortic hematopoietic stem/progenitor cell (HS/PC) generation during EHT.[12] This deficiency could be rescued by zebrafish *gpr56* (also mouse *Gpr56*) messenger RNA (mRNA) injection. Thus, *gpr56* is necessary for zebrafish aortic HS/PC development.[12] In contrast, although *Gpr56* is highly expressed by mouse HS/PCs,[25] 1 mouse germline *Gpr56* (exon2-3) deletion study showed surprisingly small changes in hematopoietic progenitor cell (HPC) numbers and HSC-repopulating activity,[25] whereas another[26] showed reduced HSC self-renewal. Because some Gpr56 protein was detected in this mouse model (possibly a failure to delete the S4 splice variant[25]), a role for Gpr56 in normal mammalian hematopoietic development remains controversial.

Here, we examine the role of Gpr56 in vivo and in vitro during mouse hematopoietic development. We show that in vivo transplanted *Gpr56* conditional knockout mouse fetal liver (FL) HSCs and *Gpr56*$^{-/-}$ mouse embryonic stem cell (ESC)-derived HPCs are myeloid-biased, that mouse *Gpr97* mRNA can rescue HS/PC generation in *gpr56* morphant zebrafish embryos, and that deletion of *Gpr56* in mouse FL HSCs and ESC-derived HPCs results in upregulated *Gpr97* expression. Deletion of both *Gpr56* and *Gpr97* in mouse ESC results in almost complete loss of HPC production, revealing previously unrecognized and important redundant roles for these 2 GPCRs in mouse hematopoietic development.

Materials and methods

Mice

Gpr56fl,[27] *VavCre*,[28] and *VECCre*[29] mice were maintained and embryos generated by mating *Gpr56fl*(C57BL/6) and *VavCre:loxGpr56* or *VECCre:loxGpr56* (C57BL/6HsdJOla) mice (2-6 months). Vaginal plug discovery was embryonic day 0 (E0). Staging was by somite counts. Ly5.1 mice (B6.SJL-*Ptprc*^{a}*Pepc*^{b}/BoyCrl, 2-4 months) were transplant recipients. Mice were maintained in University of Edinburgh animal facilities in compliance with a Home Office UK Project License.

Flow cytometry

Yolk sacs (YS) and AGMs were digested (37°C, 45 minutes) in 0.125% collagenaseT1 (C0130, Sigma-Aldrich) in phosphate-buffered saline (PBS) + 10% fetal bovine serum. FL cells were dispersed (5×) through a 30G needle. YS and AGM cells were stained with CD41-eFluor450, CD31-BV605, CD16/32-PE, c-Kit-APC, and CD45-AF450 and FL with Lin^{-}Sca1^{+}c-Kit^{+} (LSK)-SLAM markers (CD3^{-}B220^{-}Gr1^{-}Ter119^{-}NK1.1^{-}CD48^{-}, Sca1^{+}cKit^{+}CD150^{+}) (supplemental Table 1) and analyzed (LSR Fortessa/FlowJo, v10; Becton Dickinson).

EBs were PBS-washed; dissociated (37°C, 5-10 minutes) in 500 μL TrypLE Express (Gibco) and anti-CD41, CD45, CD16/32 and c-Kit stained (4°C, 30 minutes). Dead cell exclusion was by Hoechst 33342 (Invitrogen) and gates set with unstained wild-type (WT) and fluorescent-minus-1 controls. Sorted cells (Aria II/Fusion/FlowJo, v10) were collected in 50% fetal bovine serum/PBS.

Hematopoietic assays

YS, AGM, ESCs or LSK-SLAM FL cells were cultured in methylcellulose (M3434, 37°C, 5% CO_2, 10 days; Stem Cell Technologies) and colony forming unit-culture (CFU-C) scored.

LSK-SLAM FL cells (1 FL/recipient or 3, 10, or 30 cells/recipient) were injected intravenously into recipients (2 × 4.5 Gy γ-irradiation). Peripheral blood was analyzed by CD45.1/CD45.2-flow cytometry (4, 16, or 23 weeks) and multilineage analysis on tissues was performed at 23 weeks. Recipients with ≥5% donor-derived cells were considered reconstituted.

Molecular analyses

DNA was extracted from individual CFU-C, ear notches, or sorted cells in polymerase chain reaction (PCR) buffer (50 mM KCl, 10 mM TrisHCl, pH 8.3, 2.5 mM $MgCl_2$, 0.1 mg/mL gelatin, 0.45% [v/v] Igepal/NP40, 0.45% [v/v] Tween20) + Proteinase K (10 mg/mL, 1 hour, 55°C) and heat-inactivated (95°C, 10 minutes); 1 μL was used for *Gpr56* PCR.

RNA was isolated (RNeasyMicroKit; Qiagen), complementary DNA synthesized (oligodT, Invitrogen; SuperScriptIII, LifeTechnologies) and reverse transcription (RT)-PCR performed with FastSybrGreen (LifeTechnologies) and primers (supplemental Table 2).

Western blotting: 10^6 ESCs were washed (2× PBS), resuspended in ice-cold RIPA buffer + protease + phosphatase inhibitors (Thermo Fisher Scientific), incubated (30 minutes, ice), sonicated, centrifuged (maximum speed, 15 minutes), and protein quantified (BSA Kit; BioRad). Samples were boiled (95°C, 5 minutes, sodium dodecyl sulfate buffer, BioRad), sodium dodecyl sulfate-polyacrylamide gel (NuSTep) separated, transferred (30 minutes, 20 V) to nitrocellulose (Amersham). Membranes were blocked (5% semiskimmed milk: Tris-buffered saline-Tween20), blotted (ON; 4°C, 1.5% for Gpr56; RT, 2 hours for β-actin; supplemental Table 1) and washed (3 × 5 minutes, Tris-buffered saline-Tween), blotted with horseradish peroxidase-conjugated secondary antibodies (RT, 1 hour) and analyzed by OdysseyFC (Li-Cor) using ImageStudioLite.

ESC cells

IB10 embyonic stem cells (*WT, G2V, G2V.56*^{KO}*, G2V.56*^{KO}*:97*^{KO}) were cultured (37°C, 5% CO_2) on irradiated mouse embryonic fibroblasts (MEFs) in ES medium; Dulbecco's modified Eagle medium (Lonza), 15% fetal calf serum (HyClone), 2 mM GlutaMAX, 1 mM Na-pyruvate, 1% P/S, 50 mM β-mercaptoethanol (all Gibco), 0.1 mM nonessential amino acids (Lonza), and 1000 U/mL LIF (Sigma-Aldrich). Cells were trypsinized and MEFs depleted by 30 minutes of incubation in Embryoid Body formation medium (Iscove modified Dulbecco medium, 15% fetal calf serum, 1% P/S. EB induction (40 rpm; 25 × 10^3cells/mL) was in EB medium, 2 mM GlutaMAX (Gibco), 50 mg/mL ascorbic acid (Sigma-Aldrich), 4 × 10^{-4} M monothioglycerol (Sigma-Aldrich), 300 mg/mL transferrin (Roche) and supplemented (day 3) with 5% proteome-free hybridoma medium (Gibco). From day 6, 100 ng/mL stem cell factor, 1 ng/mL interleukin-3, 5 ng/mL interleukin-11 (Peprotech);

from day 4, 10 μM Y-27632 ROCK inhibitor and 0.84 nM Collagen3a were added. Reagents were refreshed every other day.

Mouse *G2V.Gpr56* knockout ESCs were *CRISPR/Cas9*[30] generated (supplemental Figure 5). Guide RNAs (gRNAs) (supplemental Table 2; http://www.e-crisp.org/E-CRISP/designcrispr.html) were cloned into *pSp-Cas9(BB)-2A-GFP* (Addgene: 48138). Mouse *G2V* ESCs[31,32] were transfected (DreamFect, OZBiosciences), GFP^+ cells seeded on MEFs at 48 hours, expanded, and screened. Mouse *G2V.Gpr56* cells were used for generating the Gpr97 knockout ESCs (supplemental Figure 6).

Zebrafish

Zebrafish (*Danio rerio*) embryos were raised at 28.5°C.[12] Heterozygous *6.0itga2b:EGFP* (CD41-GFP[33]) and *-0.8flt1:RFP* (Flt1:RFP)[34] zebrafish were maintained by crosses with WT. Embryos imaged on a LeicaSP5. All mRNA in vitro expression constructs were generated by amplification of complementary DNA with specific primers (supplemental Table 2). PCR products were cloned (*p-GEM-T*), sequence verified, and mRNA generated (Ambion sp6/T7 kit). Antisense morpholino against the splice site of the second intron (supplemental Table 2; Gene Tools) was dissolved in Milli-Q water to 1 mM (1 nL MO was injected in a 1/5 concentration in 0.1 M KCl and phenol red). For mRNA rescue experiments, 1 nL of 50 ng/μL mRNA and 200 μM was injected.

Statistical analysis

Graphs were generated using GraphPadPrism. One-way analysis of variance corrected by Bonferroni test was used to compare >2 groups, and the Student *t* test for 2-group comparisons. The Fisher exact test determined nonrandom associations in lineage-bias analysis (*$P \leq .05$, **$P \leq .01$, ***$P \leq .001$).

Results

Gpr56 conditionally deleted embryos have fewer YS hematopoietic progenitors

A conditional knockout (cKO) approach was taken to delete all isoforms (exons 4, 5, 6) of *Gpr56*[27] in mouse embryonic cells expressing *vascular endothelial-cadherin (VEC)* or *Vav* before and following HSC generation, respectively. YS isolated from E9 *VECCre:loxGpr56* cKO and WT littermates (Figure 1A) contained equivalent cell numbers (supplemental Figure 1A). $CD31^+$ cKO YS cells showed a significant decrease in relative *Gpr56* mRNA compared with WT (Figure 1B); *Gpr56* deletion was verified by DNA-PCR (supplemental Figure 1B, top). In vitro CFU-C assays revealed a significantly lower number of HPCs (CFU-C/YS) in the cKO compared with WT (Figure 1C) and 18/19 individual cKO colonies showed both *Gpr56* alleles recombined (supplemental Figure 1B, bottom). $cKit^+$ cell percentages were significantly decreased in cKO YS compared with WT, but only slight reductions were found in the percentages of erythromyeloid progenitor (EMP; $CD41^+cKit^+CD16/32^+$) and other ($CD31^+cKit^+$, $CD45^+cKit^+$) cells (Figure 1D; supplemental Figure 1C).

E9 AGM cells from this cohort of *VECCre:loxGpr56* cKO embryos were significantly reduced in $cKit^+$ cell percentages and showed slight reductions in EMPs and other progenitors (supplemental Figure 1D). In contrast, E10.5 *VECCre:loxGpr56* cKO AGM cells had no reductions in percentages of $cKit^+$, EMPs, or other progenitor cells (supplemental Figure 1E). E10.5 *VavCre:loxGpr56* cKO AGM cells ($CD41^{lo}/CD45^+$; Figure 1E; supplemental Figure 1F) were similarly examined. A significant decrease in relative *Gpr56* mRNA was found in the cKO cells compared with WT (Figure 1F). *Gpr56* deletion was verified by DNA-PCR (supplemental Figure 1G). Although there appears to be a trend toward reduced CFU-C numbers in $CD41^{lo}/CD45^+$ cKO AGM cells, it was not significant (Figure 1G) and the percentages of phenotypic hematopoietic cells in the E10.5 cKO AGM were unchanged (Figure 1H). Together, these data indicate that loss of Gpr56 affects HPCs in the E9 YS, but has little to no effect on E10.5 AGM hematopoiesis.

Hematopoietic function in E13.5 *Gpr56* cKO fetal liver

To examine whether Gpr56 loss affects FL definitive HSCs and HPCs, LSK-SLAM cells were isolated from E13.5 *VavCre:loxGpr56* and *VECCre:loxGpr56* cKO embryos (Figure 1I). *Gpr56* transcripts were reduced in cKO cells compared with WT (Figure 1J) and *Gpr56* deletion was confirmed (supplemental Figure 2A, top). The frequency of cKO HPCs (CFU-C/100 LSK-SLAM; Figure 1K) and number of LSK-SLAM cells per E13.5 FL (Figure 1L) in cKO lines were unchanged as compared with WT. A total of 14/14 individual CFU-Cs tested from *VavCre:loxGpr56* FL (supplemental Figure 2A, bottom) and 28/29 colonies from *VECCre:loxGpr56* FL (supplemental Figure 2B) showed both *Gpr56* alleles recombined. Thus, *Gpr56* is dispensable for FL HPC growth and function.

E13.5 FL *VavCre:loxGpr56* cKO LSK-SLAM cells were examined for HSC activity by in vivo transplantation (Figure 2A). Adult irradiated recipients injected with 1 FL-equivalent of LSK-SLAM cells (~100 HSCs[35]) from cKO and WT donors showed no difference in the percentage of mice engrafted or peripheral blood (PB) donor-chimerism (4 and 16 weeks postinjection; Figure 2B). Donor chimerism in the bone marrow (BM), spleen (Sp), thymus (Thy), and lymph nodes (LN) of cKO recipients at 18 weeks (Figure 2C) was equivalent to WT. Thus, Gpr56 appears dispensable for engraftment by large numbers of FL HSCs.

Clonal transplantation reveals a role for Gpr56 in FL HSC lineage bias

To test if Gpr56 affects HSC quality in clonal in vivo transplantation, 3, 10, and 30 LSK-SLAM FL cells from E13.5 *VavCre:loxGpr56* and WT littermates were transplanted (Figure 2D). Injection of 3 LSK-SLAM cells failed to reconstitute. Injection of 10 or 30 WT cells led to long-term (23-week) reconstitution (≥5% donor chimerism) in 75% (12/16) of recipients, whereas only 50% (8/16) of recipients receiving cKO cells showed reconstitution. The average percentage PB donor chimerism in recipients of 30 cKO cells (at 16 and 23 weeks) was significantly decreased compared with WT, as was the donor chimerism in the BM, spleen, LN, and Thy (Figure 2E). *Gpr56* transcripts were decreased in $CD45.2^+$ LSK cells from the BM (Figure 2F), confirming Gpr56-related HSC dysfunction.

The donor-derived lymphoid-myeloid ratio[36] was examined in the PB of cKO and WT E13.5 LSK-SLAM FL reconstituted recipients at 23 weeks (Figure 2G). Lineage output was determined by B plus T lymphoid cell percentages to granulocyte plus macrophage percentages ($B+T^{value}/G+M^{value}$), with ratios of >10, 10 to 3, and 3 to 0 considered lymphoid-biased, balanced, or myeloid-biased, respectively (Figure 2H). The 12 WT HSC recipients showed 5 with lymphoid-biased and 7 with balanced outputs. In contrast, the 10 cKO HSC recipients showed 1 lymphoid-biased,

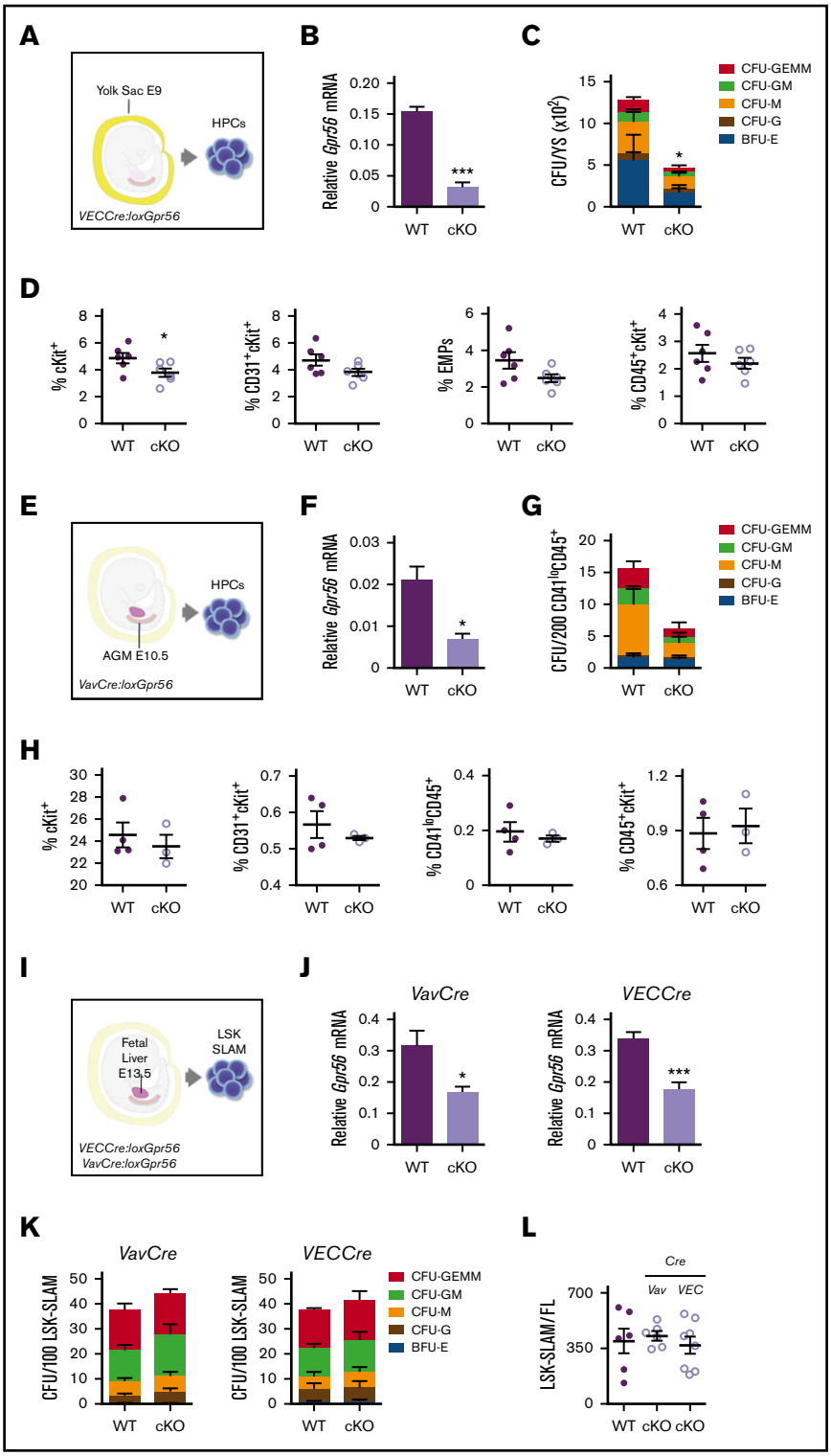

Figure 1. Gpr56 deficiency effects early hematopoietic development in mouse embryos. Experimental setup for E9 YS (21-25 somite pairs) (A), E10.5 AGM (34-37 somite pairs) (E), and E13.5 FL HPC analyses (I). (B) Relative expression of *Gpr56* in WT and *VECCre:loxGpr56* cKO E9 YS cells normalized to *β-actin* by RT-PCR analysis (n = 3). (C) Number of CFU per WT and cKO E9 YS (n = 3). (D) Percentages of cKit$^+$, CD31$^+$cKit$^+$, CD41$^+$cKit$^+$CD16/32$^+$ (EMP), and CD45$^+$ckit$^+$ cells in WT and cKO E9 YS (n = 6). Flow cytometric gating strategy shown in supplemental Figure 1. (F) Relative expression of *Gpr56* in WT and *VavCre:loxGpr56* cKO E10.5 AGM cells normalized to *β-actin* by RT-PCR analysis (n = 3). (G) Number of CFU per WT and cKO E10.5 AGM (n = 3). (H) Percentages of cKit$^+$, CD31$^+$cKit$^+$, CD41^{lo} CD45$^+$, and CD45$^+$ckit$^+$ cells in WT and cKO E10.5 AGMs (n = 6). (J) Relative expression of *Gpr56* in WT and *VavCre:* and *VECCre:loxGpr56* cKO LSK SLAM sorted E13.5 FL cells normalized to *β-actin* by RT-PCR analysis (n = 5). *$P \leq .05$. (K) Number of CFU per WT and *Vav* and *VECCre* cKO E13.5 FL LSK SLAM cells (n = 4). (L) Number of LSK SLAM cells per WT and *Vav* and *VECCre* cKO E13.5 FL (n = 6). Distinct colony types are indicated. Mean ± standard error of the mean (SEM) is shown.

5 balanced, and 4 myeloid-biased (Figure 2H). The increase in myeloid-biased HSCs was significant (Figure 2I). The BM cell lineage output of some of this cohort (supplemental Figure 2C-D) showed a similar but not significant myeloid bias in cKO HSC recipients. These data suggest that Gpr56 maintains the in vivo quality of HSCs, preserving lymphoid-biased and balanced HSC lineage output.

Gpr56 is expressed in ESC-derived hematopoietic cells

To further examine Gpr56 during development, we used *Gata2Venus* (*G2V*) mouse reporter ESCs,[31] which facilitate the isolation of HS/PCs in the Venus-expressing (V$^+$) cell fraction[31,32] (Figure S3; gating and fluorescent-minus 1). *G2V* ESCs were differentiated and

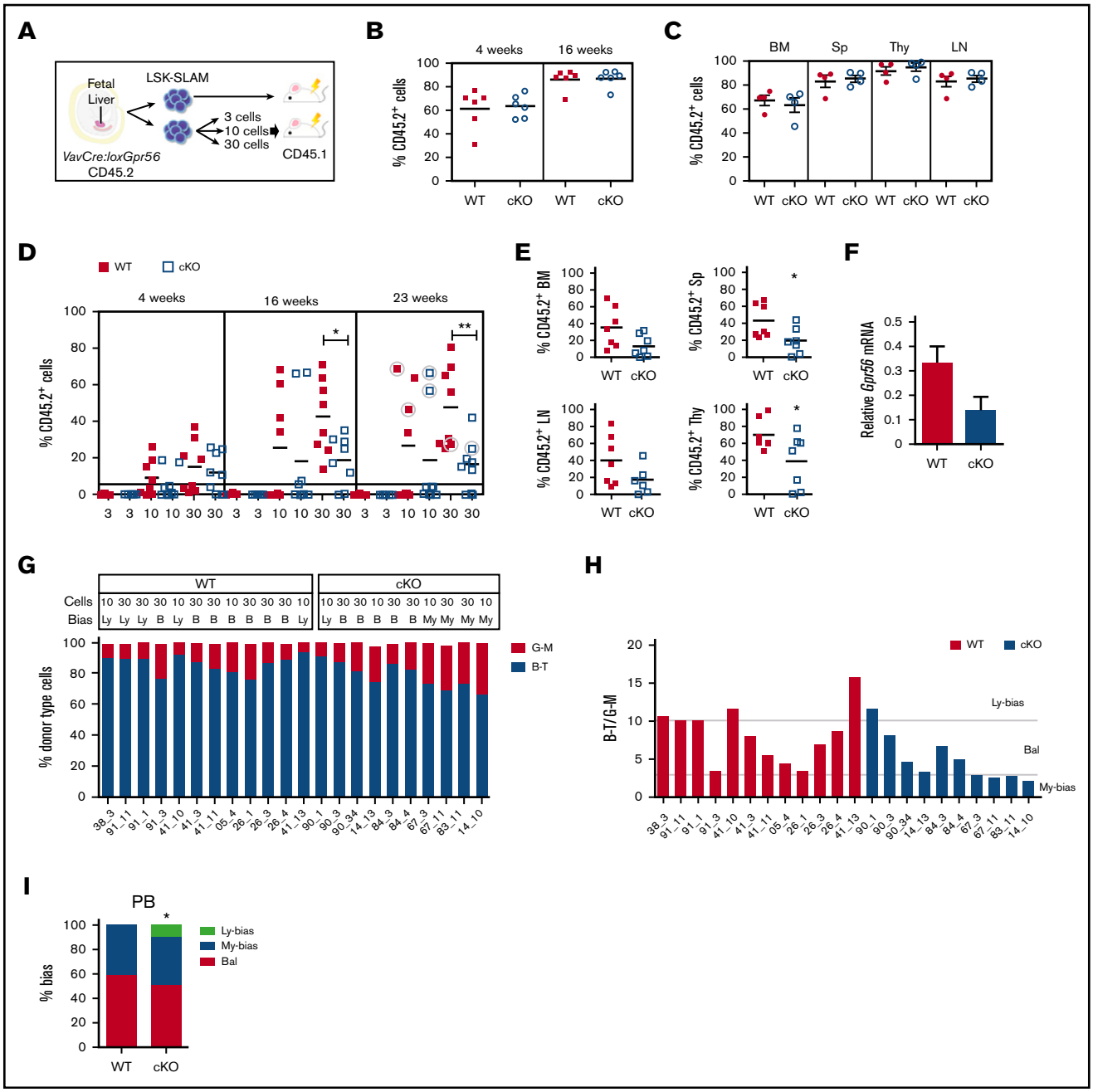

Figure 2. Clonal LSK SLAM fetal liver cell in vivo transplantations reveal decreased engraftment levels and myeloid-lineage bias for Gpr56 deficient HSCs. (A) Experimental setup for in vivo transplantation of E13.5 FL-sorted LSK SLAM cells. (B-C) One FL equivalent of LSK SLAM sorted E13.5 cells from WT and *VavCre:loxGpr56* cKO embryos (Ly5.2) were injected into adult irradiated recipients (Ly5.1). Donor cell chimerism in recipient PB at week 4 and 16 posttransplant (B) and hematopoietic tissues at week 18 posttransplant (C). Analysis is by Ly5.1/Ly5.2 flow cytometry. Mean ± SEM is shown. n = 6 per group. (D) Limiting dilution clonal HSC transplantation. Percentage of donor cell engraftment of individual adult irradiated recipient mice as measured by Ly5.1/Ly5.2 flow cytometry of PB at 4, 16, and 23 weeks postinjection of 3, 10, and 30 LSK SLAM E13.5 FL cells. WT controls (red squares) and *VavCre:loxGpr56* knockout (cKO, blue empty squares). n = 8 per group. Horizontal line at 5% indicates cutoff for reconstitution. Horizontal lines indicate average percentage engraftment. Circled individual symbols indicate mice used for secondary transplantations. *$P \leq .05$; **$P \leq .01$. (E) Percentage of donor cell engraftment at 23 weeks postinjection as measured by Ly5.1/Ly5.2 flow cytometry of BM, Sp, LN, and Thy cells from 7 recipient mice injected with 30 LSK-SLAM FL cells. *$P \leq .05$. (F) RT-PCR relative expression of *Gpr56* normalized to *β-actin* in LSK BM cells from primary recipients injected with WT and *VavCre:loxGpr56* cKO sorted E13.5 FL cells (n = 5). Mean ± SEM are shown. (G) Percentage of lymphoid and myeloid cell contribution in PB of 22 individual adult irradiated recipient mice as measured by flow cytometry of peripheral blood at 23 weeks postinjection of 10 and 30 LSK-SLAM WT control and *VavCre:loxGpr56* cKO E13.5 FL cells. (H) Ratio of B-T lymphoid and G-M myeloid for cohort of recipients in panel G with indicators for limits of lymphoid-biased, balanced and myeloid-biased HSC outputs. B, balanced; Ly, lymphoid bias; My, myeloid bias. >87% B-T=Ly; 75% to 87% B-T=B; <75% B-T=My. (I) Percentages of lymphoid-biased, balanced and myeloid-biased HSC engrafted recipients from panel H. Fisher exact test determined statistically significant differences in the My-bias fraction. *$P \leq .05$.

harvested at several time points (Figure 3A). RT-PCR analysis on cells from day 0, 6, 10, and 12 cultures showed significant increases in *Gpr56* transcript levels, peaking at day 10 and day 12 in unsorted (supplemental Figure 4A) and V^+ cells (supplemental Figure 4B). A low level of *Gpr56* expression was found in nonhematopoietic V^- cells, as expected.[16] Western blotting of whole cell extracts from unsorted differentiated *G2V* ESCs showed high-level Gpr56 protein expression at day 12 compared with day 0 (supplemental Figure 4C, left) and in day 12 V^+ compared with V^- cells (supplemental Figure 4C, right). Thus, *G2V* ESCs are a suitable platform to examine the role of Gpr56.

Gpr56 deletion affects hematopoietic output during ESC differentiation

Gpr56 deleted *G2V* ESC lines (56^{KO}) were generated by *CRISPR/Cas9* editing. gRNAs to exon 2 (common to all transcript variants; supplemental Figure 5A) were cloned (*pSP-Cas9-2A-GFP*) and transfected into *G2V* ESCs (supplemental Figure 5B). At 48 hours posttransfection, ~10% of *G2V* ESCs were GFP^+ (supplemental Figure 5C-D). Undifferentiated *G2V* clones (#5, #21) showed a complete lack of Gpr56 protein (supplemental Figure 4D) compared with WT (#1, #2). The total absence of *Gpr56* transcripts in clone #5 compared with WT ESC was verified during timecourse in vitro differentiation (supplemental Figure 4E), confirming the successful knockout of *Gpr56*.

Phenotypic HPC[37] and CFU-C analyses were performed on cells from day 6 (Figure 3B,D,F) and day 10 (Figure 3C,E,G) 56^{KO} and WT ESC cultures. The percentage of V^+ cells in both the day 6 and day 10 56^{KO} (#5 and #21) cultures was significantly increased (2.8 ± 0.95 fold) compared with WT (Figure 3D-E). Despite this increase, at day 6, a significant decrease in the percentage of $cKit^+$ (#5) and $cKit^+CD41^+$ cells in the V^+ fraction (#5 and #21) of 56^{KO} cultures was found compared with WT (Figure 3D). In contrast, at day 10, a significant increase in $cKit^+$ (#5 and #21; 1.3 ± 0.2) and phenotypic EMP percentages (#21; 1.82 ± 0.1) was found (Figure 3E).

When day 6 V^+ cells were tested for HPC function (Figure 3F), both 56^{KO} clones were significantly reduced (fourfold) in CFU-C/10^4 V^+ cells compared with WT. The significant decrease was in CFU-erythroid and CFU-megakaryocyte (CFU-M). In contrast, V^+ cells from day 10 56^{KO} (#5, #21) cultures (Figure 3G) revealed a trend ($P = .33$, $P = .68$) toward increased CFU-C/10^4 cells compared with *WT* V^+ cells. Significant increases in CFU-granulocyte (CFU-G), CFU-macrophage (CFU-M), and CFU granulocyte–macrophage (CFU-GM) frequencies for clone #5 were observed. Hence, the reduction in day 6 early HPCs and the contrasting increase in myeloid lineage progenitors at day 10 of 56^{KO} ESC differentiation agrees with in vivo *Gpr56* cKO results and suggests that Gpr56 plays distinct roles during hematopoietic development/differentiation.

In the developing brain, Col3a1 is a Gpr56 ligand[15,27] and Gpr56 signals intracellularly through Rho/ROCK.[16] To test these routes of activation in hematopoietic cells, Col3a1 or ROCK inhibitor Y-27632 were added to in vitro differentiating *G2V* ESCs. Cultures (day 12) showed no changes in the number of ESC-derived V^+ hematopoietic cells for either condition (Figure 4A). When HPC activity was analyzed, a trend toward reduced total CFU-C numbers was found with the ROCK inhibitor, whereas an increased trend was found with Col3a1 (Figure 4B). Examination of specific colony types revealed a significant increase in CFU-M and CFU granulocyte, erythroid, megakaryocyte (GEMM) in the presence of Col3a1 (Figure 4C). The ROCK inhibitor decreased burst forming unit-erythroid (BFU-E), CFU-M, and CFU-GM (Figure 4C). Our single-cell RNAseq dataset[38] of HSCs, HPCs, and endothelial cells in E10.5/11.5 intra-aortic cluster ($CD31^+G2V^{med}cKit^{hi}$) was examined for *Col3a1*, *Gpr56*, and *Arrb2*[39,40] (effector of Gpr56 activation) (Figure 4D). *Gpr56* was found highly expressed in the hematopoietic cluster (HC1) whereas *Col3a1* was highly expressed in the endothelial-like cluster. *Arrb2* was expressed at varying levels in both. These data agree with published expression analysis of AGM hematopoietic and niche populations[41] and support the notion that Col3a1 could be a ligand for Gpr56 in hematopoietic development.

Mouse *Gpr97* rescues HS/PC generation in zebrafish *gpr56* morphants

The discrepancy between the essential role for *Gpr56* in zebrafish HS/PC development and the rather minor role in the mouse was puzzling.[12] In the mouse, 3 closely related *Gpr* genes (5′-*Gpr114; Gpr56;Gpr97*-3′) are contained within a single 122-Kb locus. In zebrafish *gpr56* and *gpr97* are separated by 36 Mb (Figure 5A). Because mouse *Gpr97* and *Gpr114* are highly homologous to *Gpr56*, they may compensate for *Gpr56* loss. To test for functional redundancy, mouse (m)*Gpr56*, *Gpr97*, and *Gpr114* mRNA was injected into zebrafish embryos along with *gpr56* morpholino (MO) (Figure 5B-C). Morphant *gpr56* embryos co-injected with *zgpr56*, m*Gpr56* and m*Gpr97* mRNA showed hematopoietic rescue as quantitated by *cmyb* in situ hybridization signal, whereas mouse *Gpr114* mRNA did not. Additionally, transgenic zebrafish embryos (*CD41GFP:Flt1RFP* report HS/PC generation) were injected with the *gpr56* MO alone or in combination with *zgpr56* or m*Gpr56*, m*Gpr97*, or m*Gpr114* RNA. Double expressing $CD41^{dim}Flt1^+$ (GFP^+RFP^+) HS/PCs in the caudal hematopoietic cell tissue at 48 hpf were counted (Figure 5D-E). Significant increases in the average number of HS/PCs were found in the morphants injected with *zgpr56*, m*Gpr56*, and m*Gpr97* mRNA vs control morphants, and HS/PC numbers were equivalent to those in noninjected controls. m*Gpr114* mRNA did not restore production of HS/PC. Alignment comparisons revealed a high degree of homology between mouse Gpr97 and both zebrafish gpr56 and mouse Gpr56 in all 4 protein domains (Figure 5F), suggesting that Gpr97 may function redundantly in the mouse embryos in the absence of Gpr56.

Gpr97 expression is upregulated in the absence of *Gpr56* in vivo and in vitro

Mouse *G2V.WT* ESCs examined by *Gpr97* RT-PCR during in vitro hematopoietic differentiation showed significantly increased expression from day 6 to day 12 in the V^+ fraction (supplemental Figure 4F). Violin plots generated from single-cell RNA sequencing datasets of enriched AGM HS/PCs[38] (Figure 5G) show high expression of *Gpr56* in the 85 $CD27^+$ cells in HC1. These cells separate into 3 subclusters (A, B, C), with cluster B containing all HSC activity.[38] Compared with *Gpr56* logExp, *Gpr97* transcripts are 10-fold lower in A and 100-fold lower in B, and *Gpr114* transcripts are barely detectable. Spring analysis (Figure 4D) shows coexpression of *Gpr97* in many *Gpr56*-expressing cells in HC1, with only very few coexpressing *Gpr114*. Thus, low *Gpr97*

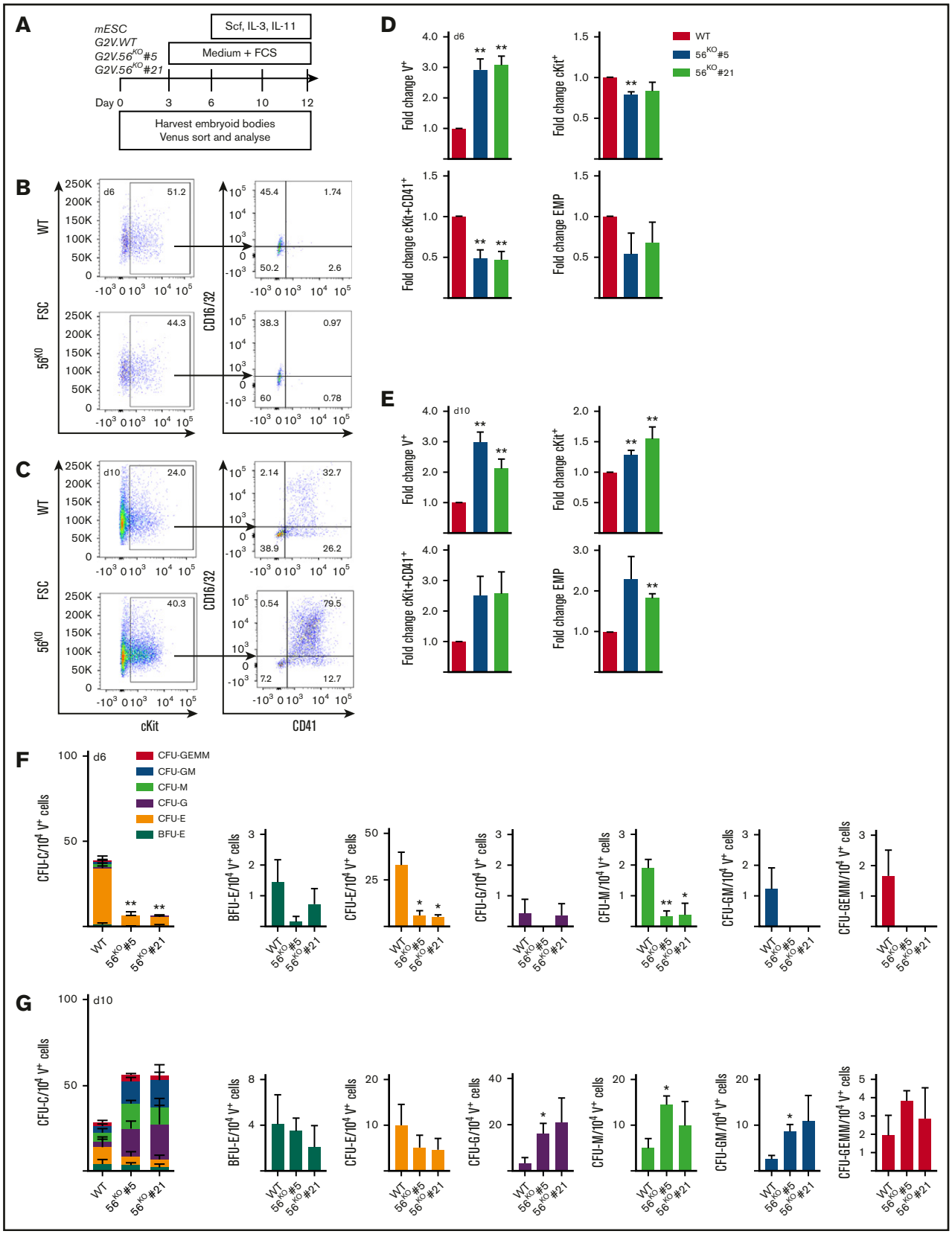

Figure 3. Gpr56 affects hematopoietic output in vitro. (A) ESC differentiation culture methodology. Mouse *Gata2Venus (mG2V)* ESC (WT and *56*^{KO}) were differentiated in hematopoietic factor-containing medium for several days and unsorted/sorted V^{+} and V^{-} cells were examined for *Gpr56* mRNA (RT-PCR) and Gpr56 protein (WB, western blot) expression. (B-C) Representative flow cytometric plots of day 6 (B) and day 10 (C) *G2V.WT* and *G2V.56*^{KO} differentiation cultures showing percentages of CD16/32 and

expression overlaps with high *Gpr56* expression in some enriched HS/PCs in mouse intra-aortic hematopoietic clusters (IAHCs).

Gpr97 levels were examined in in vitro differentiated *Gpr56*^{KO} ESCs (Figure 5H) and in vivo *VECCre:loxGpr56* and *VavCre:loxGpr56* cKO YS, AGM FL, and BM hematopoietic cells (Figure 5I). When compared with differentiated WT G2V.ESCs, significantly increased expression of *Gpr97* expression was found in the day 10 (but not day 6) V$^+$ fraction. E9 YS CD31$^+$ cells and E10.5 CD41^{lo}/CD45$^+$ AGM cells showed similar levels of *Gpr97* expression in WT and *Gpr56* cKO cells. In contrast, E13.5 FL LSK-SLAM cells showed a significant upregulated expression of *Gpr97* in *Gpr56* cKO (~1.5-fold) vs *WT* cells. The donor-derived LSK BM cells from transplant recipients of 10 or 30 cKO E13.5 LSK-SLAM FL cells showed comparable levels of relative *Gpr97* expression to WT LSK BM cells. Thus, Gpr97 may function redundantly in the definitive stage of hematopoietic development both in vitro (day 10) and in vivo (FL), but not in early development or in BM of transplant recipients.

Deletion of both *Gpr56* and *Gpr97* impairs ESC-derived hematopoiesis

To explore the functional contribution of Gpr97 during in vitro differentiation upon loss of *Gpr56*, we generated a mouse *G2V.56*^{KO}*97*^{KO} ESC line (Figure 6A; supplemental Figure 6). *CRISPR/Cas9* editing with gRNAs targeting *Gpr97* exons 2 and 10 was used to knockout all potential isoforms and/or decay RNA transcripts. Clone B3 (*56*^{KO}*97*^{KO}) was used for further studies. The absence of *Gpr97* transcripts in B3 (days 6 and 10) cells was confirmed by RT-PCR (Figure 6B). When the hematopoietic output of day 10 *56*^{KO}*97*^{KO}, *56*^{KO}, and *WT* ESCs was examined (Figure 6C) all showed >90% viable cells (Figure 6D). The fold increase of V$^+$ cells in the *56*^{KO} cultures was significant, but *56*^{KO} *97*^{KO} cultures showed no significant changes in V$^+$ cells compared with WT (Figure 6D). However, significant fold decreases in CD45$^+$ cells and CD41$^+$cKit$^+$CD16/32$^+$ (EMP) cells were observed in the *56*^{KO}*97*^{KO} differentiated cells compared with WT. This suggests that both Gpr56 and Gpr97 are involved in HPC generation and/or differentiation.

CFU-C assays were performed to quantitate HPC production in the V$^+$ fraction of day 10 *56*^{KO}*97*^{KO}, *56*^{KO}, and *WT* ESCs. In contrast to *56*^{KO} V$^+$ cells in which total CFU-C frequency was similar or slightly increased to *WT* V$^+$ cells, *56*^{KO}*97*^{KO} V$^+$ cells showed a significant large reduction in total CFU-Cs (Figure 6E). Moreover, there was a significant reduction in the frequency of *56*^{KO}*97*^{KO} -derived BFU-E, CFU-GM, and CFU-GEMM (Figure 6F) compared with *WT*. Thus, we conclude that definitive HPC production is dependent on expression of *Gpr56* and *Gpr97*.

Discussion

Our demonstration that ESC-derived definitive hematopoiesis is severely reduced in the absence of both *Gpr56* and *Gpr97* strongly supports functional redundancy in vitro in development. The knockout of *Gpr56* alone in mouse ESCs partially affects HPC production and biases output to the myeloid lineage. Moreover, *Gpr56*-deleted FL HSCs show myeloid lineage bias in vivo. Together, these data support a role for *Gpr56* in enforcing multilineage potential on HSCs in the embryo, reveal a developmental stage-dependent redundant function for Gpr97, and suggest that *Gpr97* upregulation promotes the myeloid bias of HS/PCs.

Gpr56 deletion provides new insights into the regulation of mammalian hematopoiesis

Despite the high expression of Gpr56 in quiescent adult BM HSCs,[25] the function of this adhesion-GPCR in HSCs has been controversial. Whereas a study in human leukemic cell lines and a germline *Gpr56*$^{-/-}$ mouse model claimed that EVI1-regulated *GPR56* maintains the HSC pool in BM niches,[26] others reported that this same germline knockout mouse was not impaired in BM HS/PC maintenance or function during homeostasis or stress.[25] This was suggested to be due to a hypomorphic *Gpr56* allele (low expression of S4 splice variant) or to the mouse background. Our finding of upregulated *Gpr56* expression in mouse embryo IAHC cells and the impairment of aortic HS/PC generation in *Gpr56* morphant zebrafish embryos[12] prompted examination of Gpr56 function during mouse hematopoietic development.

In our studies, *Gpr56* was conditionally deleted (exons 4, 5, 6 floxed allele[27]) in HPCs and HSCs of embryos with *VECCre* and *VavCre*. E9 YS HPC numbers were reduced, but E10.5 AGM HPC and E13.5 FL LSK-SLAM HPC and HSC numbers were unaffected. The lack of observable differences in AGM HPCs and FL HPCs and HSCs could be due to differences in recombination efficiency of VEC- and Vav-Cre in individual embryos, leading to variable amounts of residual Gpr56. Additionally, it is uncertain whether in some cases aberrant *Gpr56* transcripts are present. However, clonal in vivo transplantations of FL LSK-SLAM cells revealed qualitative changes in HSCs. In these clonal experiments, *Gpr56* loss was confirmed and affected the lineage-bias of FL HSCs. In vitro *Gpr56*^{KO} ESC hematopoietic differentiation cultures at day 6 were decreased in phenotypic and functional HPCs, similar to E9 cKO YS. However, day 10 *Gpr56*^{KO} ESCs were slightly increased in phenotypic and functional HPCs and, like E13.5 cKO FL HSCs, showed significant myeloid bias compared with the control. Hence, Gpr56 likely affects early embryonic hematopoietic generation quantitatively; at later developmental times and/or in distinct microenvironments, it has a role in HSC quality.

Gpr97 influences hematopoietic development in the absence of Gpr56

Compared with the requirement of *Gpr56* for HS/PC generation in zebrafish embryos, if Gpr56 was essential for mouse HS/PC generation, embryonic lethality would be expected. Instead,

Figure 3. (continued) CD41 cells in Venus$^+$cKit$^+$ gate. CD41$^+$cKit$^+$ CD16/32$^+$ = EMP (erythromyeloid progenitors). (D-E) Fold change in the percentages (mean ± SEM) of Venus$^+$, cKit$^+$, cKit$^+$CD41$^+$, and EMPs in day 6 (D) and day 10 (E) *G2V.WT* and *G2V.56*^{KO} (clones #5 and #21) differentiation cultures. n = 3. (F-G) Hematopoietic potential of *G2V.WT* and *G2V.56* ^{KO} (clones #5 and #21) HPCs was determined at day 6 (F) and day 10 (G) of differentiation by CFU-C assay. CFU-C per 10 000 V$^+$ plated cells is shown. Distinct colony types are indicated by color. n = 3; mean ± SEM.

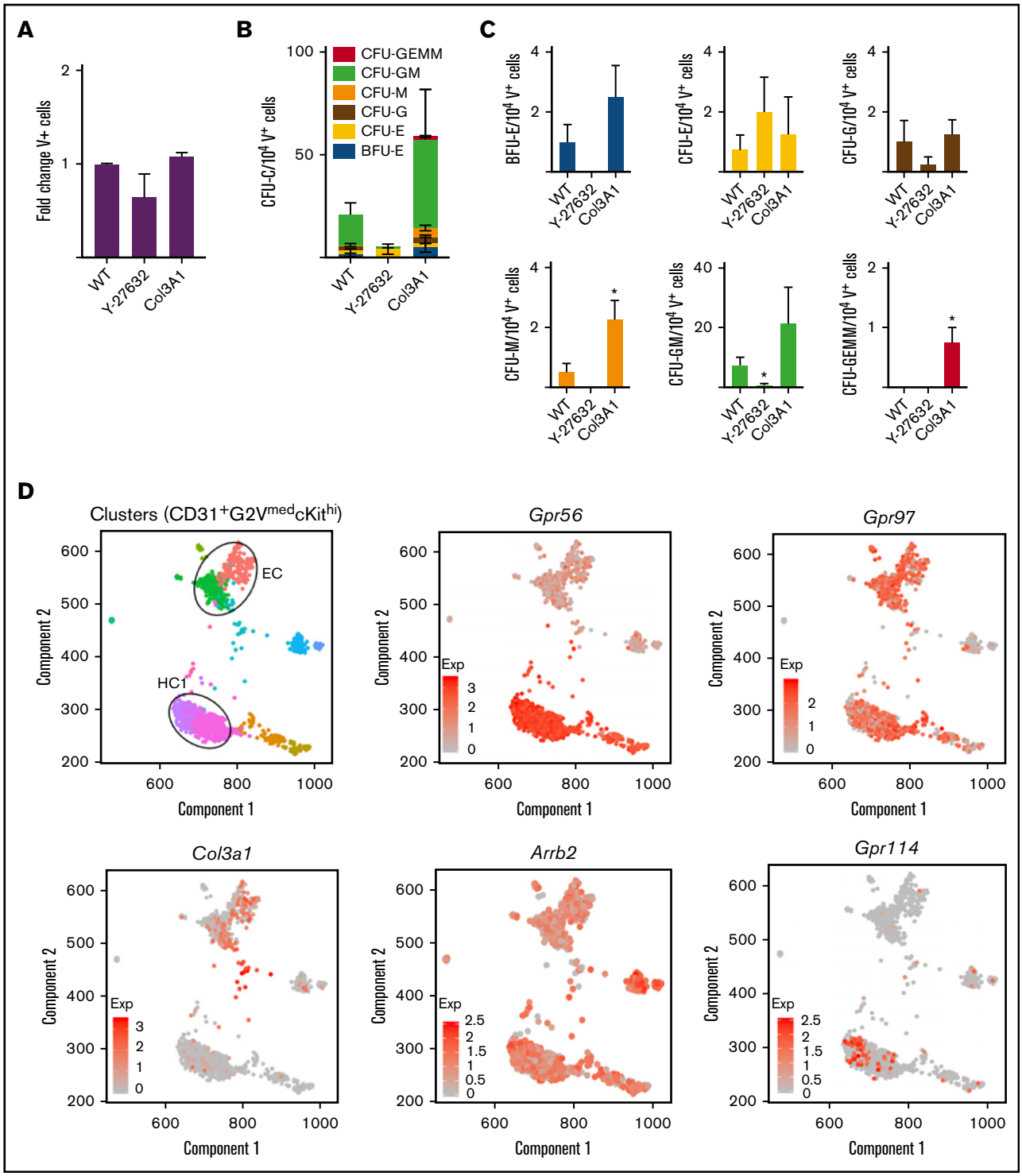

Figure 4. Functional and gene expression analyses of Gpr56 downstream effectors. (A-C) Frequency of Venus^{+} cells (A) and CFU-C colonies of day 12 V^{+} sorted cells (B-C) treated with ROCK inhibitor (Y-27632) and collagen (Col3a1). (D) Spring analysis of AGM-derived HSPCs[38] displays the differential expression of *Gpr56*, collagen (*Col3a1*), β arrestin (*Arrb2*), *Gpr97*, and *Gpr114* in the 2 cell clusters (EC and HC1) of highly enriched HSPCs (CD31^{+}G2V^{med}cKit^{hi}) from E10.5/11.5 AGM IAHC cells.

homozygous *Gpr56* mutant adults thrive and the characteristics of mutant BM HS/PCs appeared minimal.[25,26] Our rescue of *Gpr56* morphant zebrafish HS/PCs with mouse *Gpr56* and *Gpr97* mRNA raises the possibility of receptor redundancy. The linkage of *Gpr56* and *Gpr97* and the coexpression of these highly homologous receptors in the mouse, together with the loss of genomic synteny

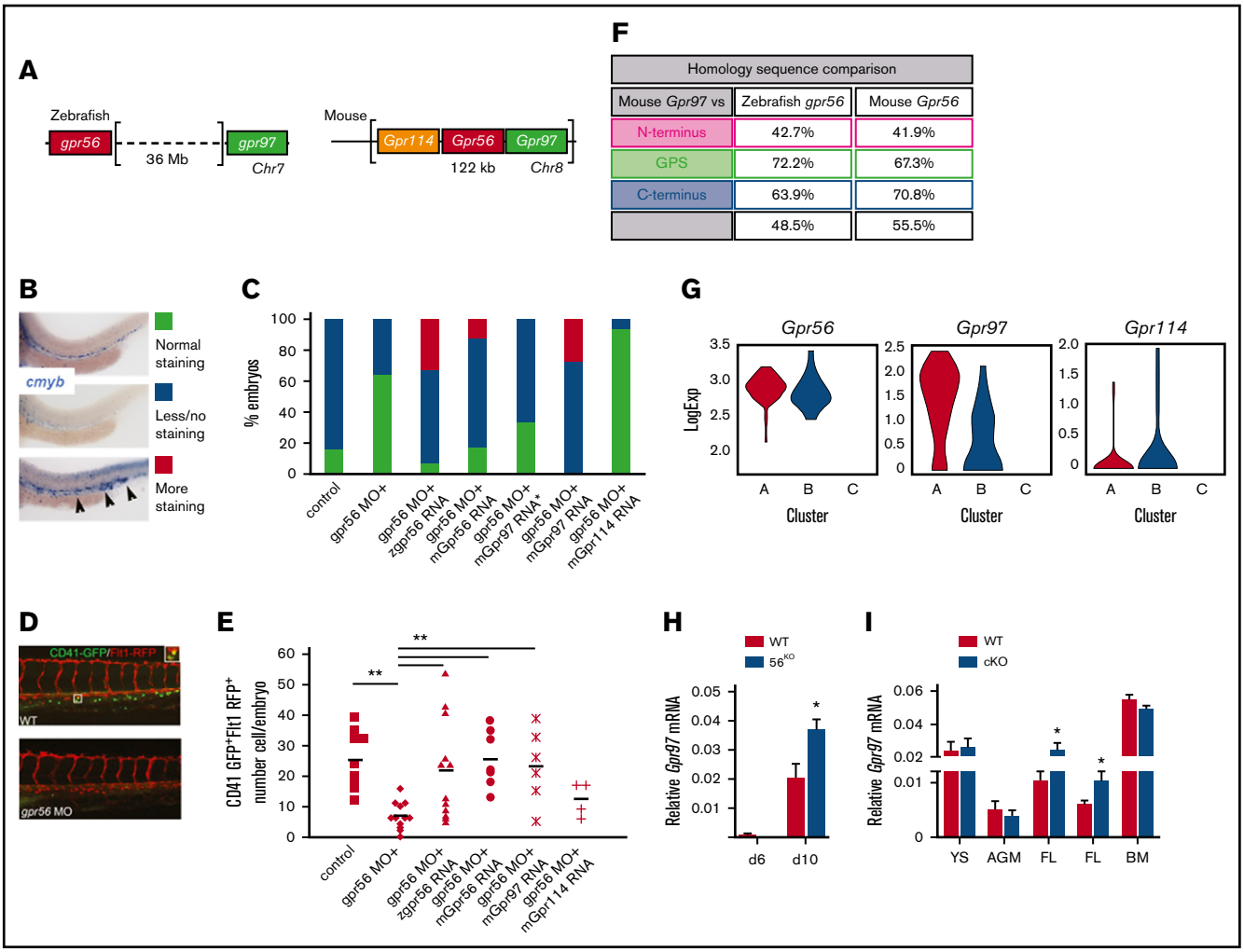

Figure 5. Redundant function of mouse Gpr97 in *Gpr56* morphant zebrafish and *Gpr97* expression in mouse ESCs and embryonic tissues. (A) Schematic of the *Gpr56* locus in zebrafish and mouse. Two highly homologous genes, *Gpr114* and *Gpr97*, are located 5′ and 3′, respectively, within the mouse *Gpr56* locus. (B) Zebrafish *cmyb* in situ staining controls (30 hpf) used for rescue experiments showing normal (green), less/no (blue), and more (red) staining. More staining was classified based on both intensity of staining compared with controls and ectopic *cmyb* expressing cells in the posterior cardinal vein and caudal hematopoietic tissue as indicated by arrowheads. (C) In situ hybridization with the HSC marker *cmyb* at 30 hpf. Histogram shows number of embryos in test groups classified as normal, less or no, and more staining. *cmyb* staining performed on zebrafish control embryos or embryos injected with *gpr56* morpholino, or *gpr56* morpholino with zebrafish (z)*gpr56*, mouse (*m*)*Gpr56, mGrp97* (30 ng*), *mGpr97*, or *mGpr114* mRNA (all with 50 ng except *). Number of experiments = 4, 4, 3, 3, 1, 1, and 1, respectively; number of embryos per condition = 92, 67, 56, 65, 15, 22, and 17. (D) Representative images of CD41GFP^{dim}Flt1RFP^{+} cells (yellow fluorescence) in the caudal hematopoietic tissue (CHT) of *gpr56* MO injected and control (WT) double transgenic zebrafish embryos at 48 hpf. CD41, green; Flt1, red; double positive definitive HS/PC, yellow (left). (E) Rescue of HS/PC production as determined by the number of CD41GFP^{dim}Flt1RFP^{+} cells in the CHT of 48 hpf control, *gpr56* morphant zebrafish, and *gpr56* morphant zebrafish injected with z*gpr56*, m*Gpr56*, m*Gpr97*, and m*Gpr114* RNA was injected. Number of experiments = 2; number of injected and analyzed embryos = 9, 12, 12, 7, 6, and 4, respectively; bars = mean; $^{**}P < .01$. (F) Percentage of amino acid sequence homology of the 4 domains of mouse Gpr97 vs zebrafish gpr56 and mouse Gpr56. (G) Violin plots showing logExp of *Gpr56, Gpr97*, and *Gpr114* in the 85 CD27^{+} cells within HC1 (Figure 4F) generated from Vink et al, 2020 single-cell RNA database.[38] HC1 CD27^{+} cells are segregated into subclusters A, B, and C. (H) RT-PCR analysis of relative *Gpr97* expression (normalized to *β-actin*) in days 6 and 10 diferentiated *G2V* WT and *G2V.56*^{KO} ESCs from hematopoietic differentiation cultures (same V^{+}cKit^{+} samples as shown in supplemental Figure 4B for relative *Gpr56* expression). n = 3. Mean ± SEM. (I) RT-PCR analysis of relative *Gpr97* expression in E9 *VECCre:loxGpr56* cKO YS cells (n = 3), E10.5 *VavCre:loxGpr56* AGM cells (n = 3), *VavCre:loxGpr56* and *VECCre:loxGpr56* cKO FL cells (n = 5 and n = 8, respectively) and LSK bone marrow cells (n = 5) from primary recipients of *VavCre:loxGpr56* cKO cells. $^{*}P \leq .05$.

in zebrafish allowed us to identify this redundancy. Importantly, *gpr97* is not expressed in the zebrafish embryos at the time of HPSC generation.[42]

Similar to mice, the human *GPR56* locus contains highly homologous *GPR114* and *GPR97* genes in the same 5′ to 3′ configuration. The evolutionary conservation of mouse and human genes/proteins, together with similarities in the embryonic development of mouse and human hematopoietic systems, suggests an overlap in the functions of Gpr56 and Gpr97. Redundancy is supported by our results showing *Gpr97* expression in cells of E9 YS, E13.5 FL, and adult BM, and also in cells of days 6 and 10 ESC differentiation

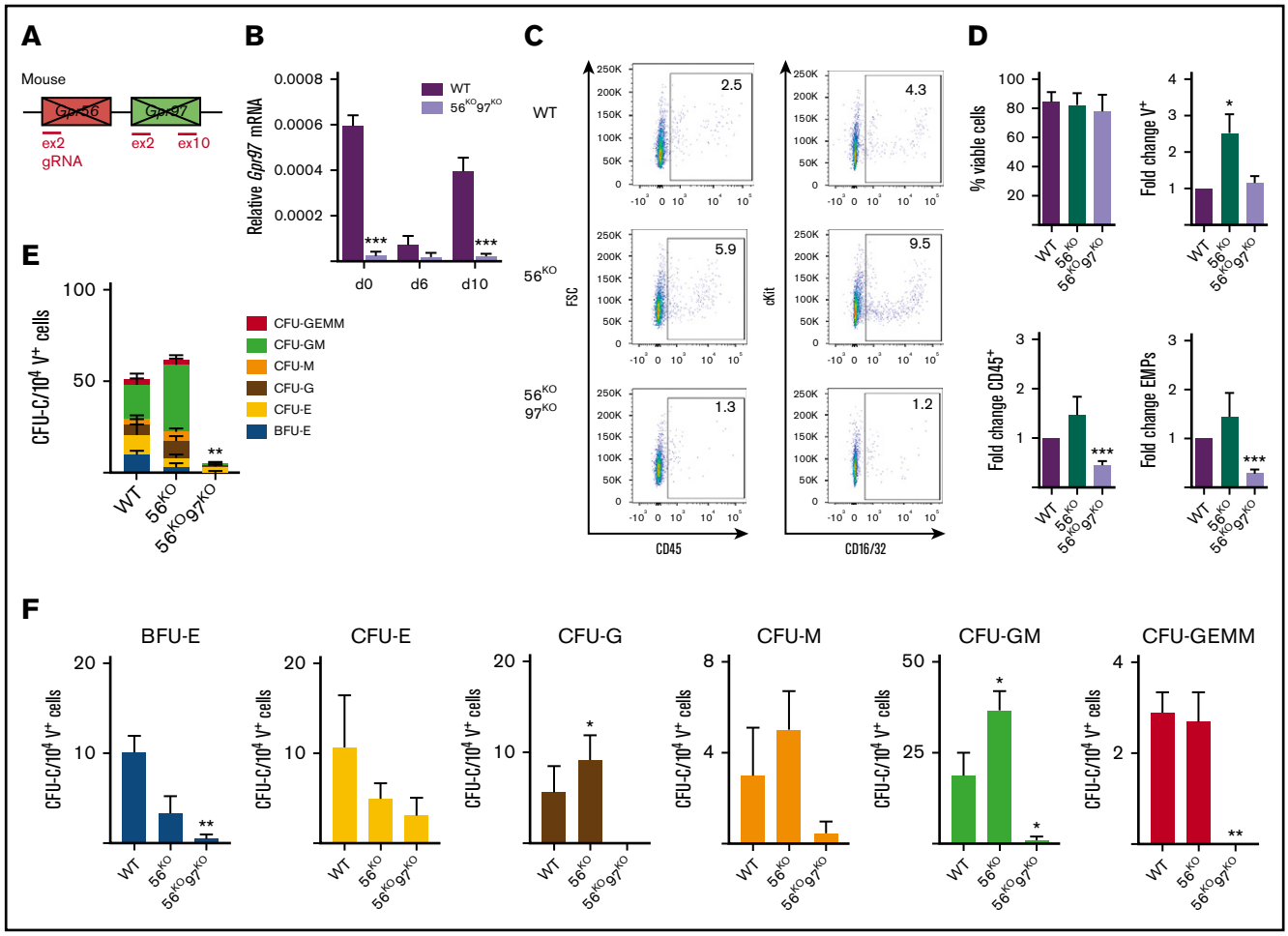

Figure 6. Decreased production of HPCs in the absence of *Gpr56* and *Gpr97*. (A) Schematic of *Gpr56* and *Gpr97* deletion in mouse *Gpr56* locus. (B) RT-PCR analysis of time course hematopoietic differentiation cultures of *G2V* WT and *G2V.56*^{KO}*97*^{KO} ESCs. Relative *Gpr97* expression (normalized to *β-actin*). (C) Representative flow cytometry plots for CD45^{+} hematopoietic cells and EMPs (CD41^{+}cKit^{+}CD16/32^{+}) from day 10 differentiated *G2V* WT, *G2V.56*^{KO}, and *G2V.56*^{KO}*97*^{KO} ESC cultures. Percentages shown in each quadrant. (D) Percentage of viable cells and fold change in percentages of V^{+}, CD45^{+}, and EMPs from day 10 differentiated *G2V* WT, *G2V.56*^{KO}, and *G2V.56*^{KO}*97*^{KO} ESC cultures. n = 3. Mean ± SEM. (E) Frequency of CFU-C in day 10 differentiated *G2V* WT, *G2V.56*^{KO}, and *G2V.56*^{KO}*97*^{KO} ESC cultures. CFU-C per 10^4 V^{+} cells is shown with colony types indicated by color. Mean ± SEM. (F) Output of CFU-C per 10^4 V^{+} in the different colony types: BFU-erythroid, CFU- E, -G, -M, -GM, -GEMM. *$P \leq .05$; **$P \leq .01$; ***$P \leq .001$.

cultures. Importantly, in the absence of *Gpr56*, *Gpr97* expression was upregulated in E13.5 FL LSK SLAM cells and day 10 differentiated ESC-derived V^{+}cKit^{+} hematopoietic cells. No changes were found in *Gpr97* expression in *Gpr56* cKO E9 YS, E9 AGM, or adult BM. Thus, in the mouse embryo and only in the definitive HSC stage the loss of Gpr56 function is compensated by Gpr97.

Positive role of Gpr97 or negative role of Gpr56 for myeloid bias?

Myeloid bias was observed in cells from in vitro differentiated *Gpr56*^{KO} ESC cultures and in vivo in the recipients of *Gpr56* cKO FL HSCs. Previously, lineage-biased output of HSCs has been reported as an age-related characteristic.[43-46] As measured by long-term in vivo clonal transplantation, BM HSCs from young mice yield lymphoid-biased and balanced output. BM from aged mice show a higher frequency of myeloid-biased HSC. Our data showing the myeloid bias of *Gpr56* cKO FL HSCs support a qualitative role(s) for Gpr56 in HSC lineage output. Indeed, this qualitative property is established in midgestation mouse embryos when the first adult-repopulating HSCs are generated.[2,3] Highly upregulated *Gpr56* expression localizes to emerging E10.5/11.5 IAHC cells as they transition from endothelial cells,[12] and we show the coexpression of *Gpr97* and *Gpr56* in single highly enriched AGM HSCs.[38]

Whether Gpr56 functions to retain multipotency or represses myeloid-bias, or whether Gpr97 (especially its upregulated expression in the absence of Gpr56) activates myeloid-bias is uncertain. In human NK cells, GPR56 negatively regulates immediate effector functions.[47] Human polymorphonuclear cells highly express GPR97, whereas monocytes and lymphocytes do not.[48] These results highlight a likely balance of these GPCRs in specific subsets of hematopoietic cells as an important factor impacting cellular functions. As we have demonstrated here that

ESC-derived hematopoiesis is severely reduced in the absence of both *Gpr56* and *Gpr97*, the specific functions of these 2 closely related receptors can only be addressed through the generation of a double-knockout mouse or human cell line model. Our attempts to generate a $Gpr56^{-/-}Gpr97^{-/-}$ germline mouse have been unsuccessful, likely because of embryonic lethality. Future studies aim to understand the individual roles of these receptors during HSC development by generating a cKO model across both genes and comparing effects with single cKOs and/or individual rescue of *Gpr56* and *Gpr97*.

Acknowledgments

The authors thank A. Rossi, F. Glykofrydis, and laboratory members for assistance and critical discussions concerning this study. They acknowledge the assistance of the Queens Medical Research Institute (QMRI) Flow Cytometry facility (S. Johnston, W. Ramsay, and M. George) and the Bioresearch & Veterinary Services (BVS) service staff.

These studies were supported by European Research Council (ERC) AdG (341096), Blood Cancer UK (18010), ZonMW TOP (91211068), and the National Institutes of Health, National Institute of Diabetes and Digestive and Kidney Diseases (RO37 DK54077).

Authorship

Contribution: E.D., A.M., S.A.M., and E.d.P. conceived the project and designed the experiments; E.D. and S.A.M. directed the project; A.M., S.A.M., and E.d.P. performed the experiments; X.P. provided the *loxGpr56* mice; C.S.V. and S.A.M. performed hematopoietic transplantation experiments and A.M. and C.R.-S. performed in vitro culturing and HPC assays; M.-L.L helped generate the $Gpr56^{KO}$ embryonic stem cells; A.M. and S.A.M. generated *CRISPR/Cas9* constructs; A.M., S.A.M., and C.R.-S. performed molecular analyses; and E.D., A.M., and S.A.M. wrote the manuscript.

Conflict-of-interest disclosure: The authors declare no competing financial interests.

ORCID profiles: A.M., 0000-0003-4740-1023; S.A.M., 0000-0003-4950-0607; C.S.V., 0000-0002-3202-8361; X.P., 0000-0001-7540-6767; E.D., 0000-0001-8256-5635.

Correspondence: Samanta A. Mariani, University of Edinburgh, Centre for Inflammation Research, Queens Medical Research Institute, 47 Little France Crescent, Edinburgh, EH16 4TJ, United Kingdom; e-mail: s.mariani@ed.ac.uk; and Elaine Dzierzak, University of Edinburgh, Centre for Inflammation Research, Queens Medical Research Institute, 47 Little France Crescent, Edinburgh, EH16 4TJ, United Kingdom; e-mail: elaine.dzierzak@ed.ac.uk.

References

1. Ciau-Uitz A, Patient R. Gene regulatory networks governing the generation and regeneration of blood. *J Comput Biol*. 2019;26(7):719-725.
2. Dzierzak E, Bigas A. Blood development: hematopoietic stem cell dependence and independence. *Cell Stem Cell*. 2018;22(5):639-651.
3. Dzierzak E, Speck NA. Of lineage and legacy: the development of mammalian hematopoietic stem cells. *Nat Immunol*. 2008;9(2):129-136.
4. Jaffredo T, Nottingham W, Liddiard K, Bollerot K, Pouget C, de Bruijn M. From hemangioblast to hematopoietic stem cell: an endothelial connection? *Exp Hematol*. 2005;33(9):1029-1040.
5. Gao P, Chen C, Howell ED, et al. Transcriptional regulatory network controlling the ontogeny of hematopoietic stem cells. *Genes Dev*. 2020;34(13-14):950-964.
6. Porcheri C, Golan O, Calero-Nieto FJ, et al. Notch ligand Dll4 impairs cell recruitment to aortic clusters and limits blood stem cell generation. *EMBO J*. 2020;39(8):e104270.
7. Li Y, Gao L, Hadland B, Tan K, Speck NA. CD27 marks murine embryonic hematopoietic stem cells and type II prehematopoietic stem cells. *Blood*. 2017;130(3):372-376.
8. Lichtinger M, Ingram R, Hannah R, et al. RUNX1 reshapes the epigenetic landscape at the onset of haematopoiesis. *EMBO J*. 2012;31(22):4318-4333.
9. Moignard V, Woodhouse S, Haghverdi L, et al. Decoding the regulatory network of early blood development from single-cell gene expression measurements. *Nat Biotechnol*. 2015;33(3):269-276.
10. Swiers G, Baumann C, O'Rourke J, et al. Early dynamic fate changes in haemogenic endothelium characterized at the single-cell level. *Nat Commun*. 2013;4(1):2924.
11. Zhou F, Li X, Wang W, et al. Tracing haematopoietic stem cell formation at single-cell resolution. *Nature*. 2016;533(7604):487-492.
12. Solaimani Kartalaei P, Yamada-Inagawa T, Vink CS, et al. Whole-transcriptome analysis of endothelial to hematopoietic stem cell transition reveals a requirement for Gpr56 in HSC generation. *J Exp Med*. 2015;212(1):93-106.
13. Langenhan T, Aust G, Hamann J. Sticky signaling–adhesion class G protein-coupled receptors take the stage. *Sci Signal*. 2013;6(276):re3.
14. Zhu B, Luo R, Jin P, et al. GAIN domain-mediated cleavage is required for activation of G protein-coupled receptor 56 (GPR56) by its natural ligands and a small-molecule agonist. *J Biol Chem*. 2019;294(50):19246-19254.
15. Luo R, Jeong SJ, Yang A, et al. Mechanism for adhesion G protein-coupled receptor GPR56-mediated RhoA activation induced by collagen III stimulation. *PLoS One*. 2014;9(6):e100043.
16. Ackerman SD, Garcia C, Piao X, Gutmann DH, Monk KR. The adhesion GPCR Gpr56 regulates oligodendrocyte development via interactions with Gα12/13 and RhoA. *Nat Commun*. 2015;6(1):6122.

17. Olaniru OE, Pingitore A, Giera S, et al. The adhesion receptor GPR56 is activated by extracellular matrix collagen III to improve β-cell function. *Cell Mol Life Sci*. 2018;75(21):4007-4019.

18. Ackerman SD, Luo R, Poitelon Y, et al. GPR56/ADGRG1 regulates development and maintenance of peripheral myelin. *J Exp Med*. 2018;215(3): 941-961.

19. Cauley ES, Hamed A, Mohamed IN, et al. Overlap of polymicrogyria, hydrocephalus, and Joubert syndrome in a family with novel truncating mutations in ADGRG1/GPR56 and KIAA0556. *Neurogenetics*. 2019;20(2):91-98.

20. Piao X, Hill RS, Bodell A, et al. G protein-coupled receptor-dependent development of human frontal cortex. *Science*. 2004;303(5666): 2033-2036.

21. Daria D, Kirsten N, Muranyi A, et al. GPR56 contributes to the development of acute myeloid leukemia in mice. *Leukemia*. 2016; 30(8):1734-1741.

22. Pabst C, Bergeron A, Lavallée VP, et al. GPR56 identifies primary human acute myeloid leukemia cells with high repopulating potential in vivo. *Blood*. 2016;127(16):2018-2027.

23. Barjesteh van Waalwijk van Doorn-Khosrovani S, Erpelinck C, van Putten WL, et al. High EVI1 expression predicts poor survival in acute myeloid leukemia: a study of 319 de novo AML patients. *Blood*. 2003;101(3):837-845.

24. Gröschel S, Sanders MA, Hoogenboezem R, et al. A single oncogenic enhancer rearrangement causes concomitant EVI1 and GATA2 deregulation in leukemia. *Cell*. 2014;157(2):369-381.

25. Rao TN, Marks-Bluth J, Sullivan J, et al. High-level Gpr56 expression is dispensable for the maintenance and function of hematopoietic stem and progenitor cells in mice. *Stem Cell Res (Amst)*. 2015;14(3):307-322.

26. Saito Y, Kaneda K, Suekane A, et al. Maintenance of the hematopoietic stem cell pool in bone marrow niches by EVI1-regulated GPR56. *Leukemia*. 2013;27(8):1637-1649.

27. Giera S, Deng Y, Luo R, et al. The adhesion G protein-coupled receptor GPR56 is a cell-autonomous regulator of oligodendrocyte development. *Nat Commun*. 2015;6(1):6121.

28. Stadtfeld M, Graf T. Assessing the role of hematopoietic plasticity for endothelial and hepatocyte development by non-invasive lineage tracing. *Development*. 2005;132(1):203-213.

29. Chen MJ, Yokomizo T, Zeigler BM, Dzierzak E, Speck NA. Runx1 is required for the endothelial to haematopoietic cell transition but not thereafter. *Nature*. 2009;457(7231):887-891.

30. Ran FA, Hsu PD, Wright J, Agarwala V, Scott DA, Zhang F. Genome engineering using the CRISPR-Cas9 system. *Nat Protoc*. 2013;8(11):2281-2308.

31. Kaimakis P, de Pater E, Eich C, et al. Functional and molecular characterization of mouse Gata2-independent hematopoietic progenitors. *Blood*. 2016; 127(11):1426-1437.

32. Kauts ML, Rodriguez-Seoane C, Kaimakis P, et al. In vitro differentiation of Gata2 and Ly6a reporter embryonic stem cells corresponds to in vivo waves of hematopoietic cell generation. *Stem Cell Reports*. 2018;10(1):151-165.

33. Lin HF, Traver D, Zhu H, et al. Analysis of thrombocyte development in CD41-GFP transgenic zebrafish. *Blood*. 2005;106(12):3803-3810.

34. Bussmann J, Bos FL, Urasaki A, Kawakami K, Duckers HJ, Schulte-Merker S. Arteries provide essential guidance cues for lymphatic endothelial cells in the zebrafish trunk. *Development*. 2010;137(16):2653-2657.

35. Kim I, He S, Yilmaz OH, Kiel MJ, Morrison SJ. Enhanced purification of fetal liver hematopoietic stem cells using SLAM family receptors. *Blood*. 2006; 108(2):737-744.

36. Sieburg HB, Cho RH, Dykstra B, Uchida N, Eaves CJ, Muller-Sieburg CE. The hematopoietic stem compartment consists of a limited number of discrete stem cell subsets. *Blood*. 2006;107(6):2311-2316.

37. McGrath KE, Frame JM, Fegan KH, et al. Distinct sources of hematopoietic progenitors emerge before HSCs and provide functional blood cells in the mammalian embryo. *Cell Rep*. 2015;11(12):1892-1904.

38. Vink CS, Calero-Nieto FJ, Wang X, et al. Iterative single-cell analyses define the transcriptome of the first functional hematopoietic stem cells. *Cell Rep*. 2020;31(6):107627.

39. Kroeze WK, Sassano MF, Huang XP, et al. PRESTO-Tango as an open-source resource for interrogation of the druggable human GPCRome. *Nat Struct Mol Biol*. 2015;22(5):362-369.

40. Lefkowitz RJ, Shenoy SK. Transduction of receptor signals by beta-arrestins. *Science*. 2005;308(5721):512-517.

41. Pimanda JE, Göttgens B. Gene regulatory networks governing haematopoietic stem cell development and identity. *Int J Dev Biol*. 2010;54(6-7): 1201-1211.

42. Harty BL, Krishnan A, Sanchez NE, Schiöth HB, Monk KR. Defining the gene repertoire and spatiotemporal expression profiles of adhesion G protein-coupled receptors in zebrafish. *BMC Genomics*. 2015;16(1):62.

43. Benz C, Copley MR, Kent DG, et al. Hematopoietic stem cell subtypes expand differentially during development and display distinct lymphopoietic programs. *Cell Stem Cell*. 2012;10(3):273-283.

44. Cho RH, Sieburg HB, Muller-Sieburg CE. A new mechanism for the aging of hematopoietic stem cells: aging changes the clonal composition of the stem cell compartment but not individual stem cells. *Blood*. 2008;111(12):5553-5561.

45. Geiger H, de Haan G, Florian MC. The ageing haematopoietic stem cell compartment. *Nat Rev Immunol*. 2013;13(5):376-389.

46. Verovskaya E, Broekhuis MJ, Zwart E, et al. Heterogeneity of young and aged murine hematopoietic stem cells revealed by quantitative clonal analysis using cellular barcoding. *Blood*. 2013;122(4):523-532.

47. Chang GW, Hsiao CC, Peng YM, et al. The adhesion G protein-coupled receptor GPR56/ADGRG1 is an inhibitory receptor on human NK cells. *Cell Rep*. 2016;15(8):1757-1770.

48. Hsiao CC, Chu TY, Wu CJ, et al. The adhesion G protein-coupled receptor GPR97/*ADGRG3* is expressed in human granulocytes and triggers antimicrobial effector functions. *Front Immunol*. 2018;9:2830.